PHYSICAL REVIEW B **82**, 201403(R) (2010)

Stopping of energetic argon cluster ions in graphite: Role of cluster momentum and charge

V. N. Popok*
Department of Physics, University of Gothenburg, 41296 Gothenburg, Sweden

J. Samela and K. Nordlund
Department of Physics and Helsinki Institute of Physics, University of Helsinki, P.O. Box 43, FI-00014 Helsinki, Finland

E. E. B. Campbell
School of Chemistry, Edinburgh University, EH0 3JJ Edinburgh, Scotland, United Kingdom
and Division of Quantum Phases and Devices, Konkuk University, Seoul 143-701, Korea
(Received 25 October 2010; published 8 November 2010)

We show that the implantation depth for argon clusters in graphite scales linearly with cluster momentum. A plot of implantation depth versus the momentum scaled with the projected surface area of the cluster falls on the same universal plot as that shown for semiconductor and metallic clusters, thus providing a universal scaling law for cluster implantation. Molecular dynamics simulations provide some insight to the mechanisms behind the empirical observation.

DOI: 10.1103/PhysRevB.82.201403 PACS number(s): 68.37.−d, 79.20.Ap, 81.05.uf, 36.40.Wa

The possibility of designing and controlling the physical and chemical properties of materials on the nanoscale is currently of significant interest and there are many activities worldwide focused on this goal. Various bottom-up and top-down approaches are in use depending on the requirements. Advantages of the cluster-ion-beam method are the precise control of cluster size and cluster-surface interaction energy.[1,2] This paves the way for a number of practical applications, for example, pinning of size-selected clusters and the use of these nanostructured surfaces in electronics, for biochips[3] and for catalysis,[4] for ultrashallow junction formation and infusion doping,[1,5] and dry etching and smoothing.[1,2] It was also recently shown that deposited metal nanoparticles can be used for etching of graphene,[6,7] thus creating the possibility of novel nanoscale machining. From the application point of view, it is essential to know all the parameters that influence the cluster-surface interaction and related phenomena. The development of scaling laws provides a useful means of summarizing the most important parameters and determining the optimum experimental conditions for achieving the desired goal.

Due to the fact that a cluster is a multicomponent system with relatively weak bonding between the constituents, the cluster-surface energetic interaction is fundamentally different from that of monoatomic impact, thus causing a number of specific phenomena.[2,8] For instance, clusters require much lower energy to penetrate the surface and their constituents have longer average ranges compared to monomers at the same impact energy.[2,9,10] The primary collision between the cluster and the target atoms affects very much both the dynamics of the cluster and the subsequent relaxation phenomena in the target.[11–13] The absence of a commonly accepted theory of cluster stopping in matter complicates the use of cluster beams: different simulations and experiments show rather different dependences of the projected ranges R_p of cluster constituents and the radiation damage for various cluster species, sizes, and energies as well as for different target materials.[2] However, a recent study of metal cluster implantation in graphite indicated a very similar implantation behavior for different metal species.[7] The R_p for all studied metal clusters followed the same type of dependence when plotted against the cluster momentum scaled with the cross-sectional area of the cluster projected on the surface. This dependence is different from that of monoatomic projectiles which typically demonstrate linear scaling with energy (not momentum).[14] However, the observed behavior has some similarity to the impact of macroscopic projectiles for which the penetration depth was found to be a linear function of velocity.[15] The study of atomic cluster-surface collisions can thus contribute to a better understanding of the transition from atomic to macroscale dynamics in impact phenomena.

In this Rapid Communication, we present results of argon cluster implantation in highly ordered pyrolytic graphite (HOPG) and show that the stopping of these cluster species follows the same empirical law found earlier for metal clusters.[7] This surprising result clearly demonstrates the universal nature of the cluster stopping behavior. Molecular-dynamics (MD) simulations indicate that charge transfer and cluster deformation on impact may be important factors influencing the implantation of rare gas clusters.

Clusters of argon were produced using a cluster implantation and deposition apparatus, described previously,[16,17] and implanted into HOPG. Implantations were carried out using positively charged cluster ions of two sizes, $n=16\pm1$ and $n=41\pm2$. The mean kinetic energies varied from 1.6 up to 16.0 keV/cluster (energy per cluster atom $E_{at}=100-1000$ eV/atom) for $n=16$ and from 2.05 up to 20.1 keV/cluster ($E_{at}=50-490$ eV/atom) for $n=41$. The implantation fluence was kept low, 10^9-10^{10} cm^{-2}, in order to prevent overlapping of the impact areas and especially the corresponding etched pits.

After implantation, the samples were heated at 600 °C for approximately 10 min in a furnace under ambient atmosphere. This led to the formation of pits at the spots where the surface was damaged by cluster implantation. The depth of the etched pits is known to correspond to the depth of the radiation damage, thus providing a convenient and accurate way of measuring this.[7,18,19]

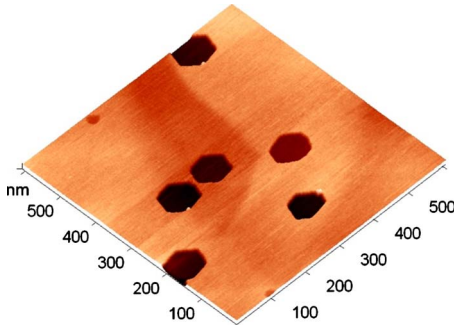

FIG. 1. (Color online) AFM image of HOPG surface after implantation of Ar_{16}^{+} cluster ions with an energy of 200 eV/atom (3.2 keV/cluster) followed by etching.

Scanning tunneling microscopy (STM) and atomic force microscopy (AFM) were used *ex situ* to study the damage made by the clusters on as-implanted samples and to measure the depth of the etched pits. The STM studies were done in constant current mode with a bias of 70–80 mV using PtIr tips. AFM measurements were carried out in tapping mode using commercial ultrasharp Si cantilevers.

Cluster ion impacts were simulated with classical MD. The main principles of the algorithms are presented in Refs. 7 and 20–22. The graphite structure was modeled using an improved Tersoff potential[23] which includes a Lennard-Jones-type interaction between graphite layers. A Lennard-Jones-type pair potential was used also for the Ar-Ar interactions and modified for the different types of simulations. A short-range repulsive force[14] was also present between all pairs of atoms to better describe collisions between them. The Ar-C interaction was purely repulsive.[23,24] The energy consumed by electronic stopping was calculated for each atom that had kinetic energy higher than 5 eV and then this electronic stopping energy was subtracted from the kinetic energy of the atom.[25] The modeling does not predict any significant influence of electronic stopping. In the simulations, a graphite surface was bombarded at normal incident angle with Ar_n clusters ($n=10$, 16, 32, and 41). Both the orientation of the impacting cluster and the impact point were varied using a random number generator. Average depths of the damaged regions were calculated from ten simulations at each size and energy. The size of the graphite box was $20\times20\times20$ nm^3, and the borders were cooled to prevent waves induced by the impact to return back to the impact region over periodic boundaries.

On the STM images of the cluster-implanted samples one can typically see tiny bumps (2–4 nm in diameter) assigned to the damage introduced by individual cluster impacts. The impact areas become clearly visible as hexagonal pits after heating-induced oxidative etching (see typical image in Fig. 1). The number of pits per unit area correlates with the implantation fluence. For the energies used for the implantation (50–1000 eV/atom), the MD simulations show that the radiation damage in graphite is produced mainly by primary nuclear stopping of the cluster constituents, the recoil radiation cascades give only a minor contribution (Fig. 2). Thus, the depth of pits corresponds not only to the depth of the radiation damage but also to R_p of the deepest cluster constituents. Sometimes, in simulations, single Ar atoms are seen to channel relatively far away from the damaged region but even if this occurs in reality these single atoms will produce only point defects and will not play any role for etching of the main damaged region, i.e., for the estimation of R_p.

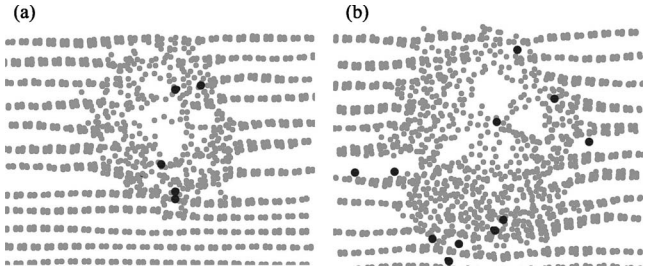

FIG. 2. Snapshots of typical simulation results: (a) 500 eV/atom Ar_{16} and (b) 500 eV/atom Ar_{41}. Ar atoms are shown in black. Width of the frames is 5 nm and they show 1-nm-thick slices, thus, most of the Ar atoms are located outside the slices and not visible.

As one can see from the dependences presented in Fig. 3(a), the depth of pits or R_p is higher for larger clusters for the same energy per atom. It also follows from the dependences that R_p increases as a function of the square root of the implantation energy, $\sqrt{E}$. Thus, R_p scales linearly with cluster momentum which is proportional to $\sqrt{E}$ but not with

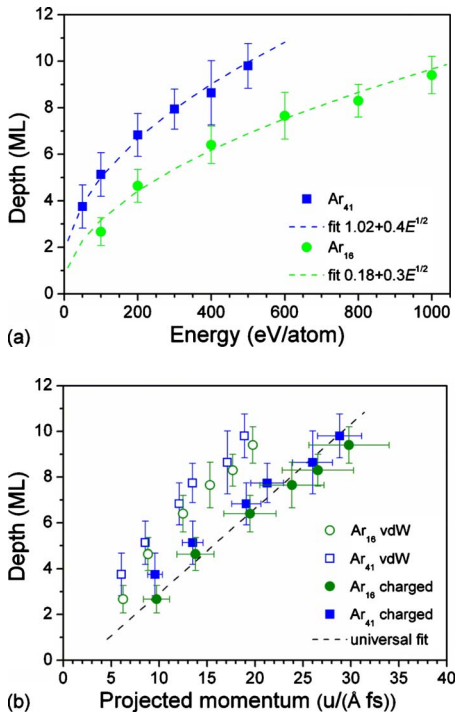

FIG. 3. (Color online) Experimentally found dependences of depth (in number of monolayers) of etched pits on (a) implantation energy, E, and (b) projected cluster momentum, p_{proj}. In (b), open symbols are calculated using the neutral cluster geometry, solid symbols are for the charged one. Vertical error bars give uncertainties of the pit depth, the horizontal ones correspond to variations in S according to the geometrical configurations as discussed in the text. Dashed lines in (a) show fittings with function $\sqrt{E_{at}}$. Dashed line in (b) represents the universal fitting line from Ref. 7.

energy as in the case of monoatomic projectiles.

It was shown elsewhere[7,19] that if the cluster momentum is divided by the cross-sectional area of the cluster S to give the scaled or projected momentum, p_{proj}, all impact data for metal and Si clusters fall on a single straight line in a plot of depth vs p_{proj}. In the case of metal clusters, a spherical cluster approximation was used to estimate S. However, this approximation does not provide a suitable approach for small rare gas clusters since the presence of charge significantly changes the cluster structure and geometrical configuration of atoms. In small argon cluster ions the charge is thought to be distributed among 3–4 core atoms leading to a large increase in binding energy.[26] Theoretical calculations show that the bond length in the ion core shrinks to approximately 2.45–2.99 Å, compared to 3.76 Å for pure van der Waals bonding in the neutral species.[27,28] The atoms surrounding the charged core become polarized thus providing an additional attractive interaction reducing the bond length and distorting the shape of the cluster. For example, the Ar_{16}^{+} cluster ion is predicted to be slightly elongated along the charged core.[28] This shape can be quite well approximated by an ellipsoid. For the $Ar_{41\pm2}^{+}$ cluster ions, we used the lowest energy geometry for the Ar_{43}^{+} cluster ion suggested in Ref. 29. The mean S values are found using the orientations of the impacting cluster giving the smallest and the largest projected areas on the surface. The dependences of depth vs p_{proj} for both sizes are presented in Fig. 3(b). For comparison, one can also see the case when the presence of charge was disregarded and S was calculated assuming van der Waals bonds. The impact data for the case when the charged cluster geometry is considered, fall very well on the single fitting line [dashed line in Fig. 3(b) $R_p=-0.79+0.37p_{proj}$] that was obtained previously for implantation of several different metal clusters, namely, Au_7, Ag_7, Ag_{13}, and Co_n ($n=30$, 50, and 63) as well as Si_7.[7] Thus, the current case of rare gas cluster ions clearly demonstrates the universality of this empirical law for cluster stopping in graphite.

MD simulations were carried out to obtain some insight into the cluster stopping mechanisms. The pair potential equilibrium Ar-Ar distance was decreased in order to simulate clusters with average geometrical cross sections corresponding to those of the charged clusters. However, these simulations overestimated the projected ranges compared to the experiment (Fig. 4) leading us to infer that some effect which is not taken into consideration in the classical MD modeling is important. Partial cluster fragmentation on impact can be such an effect: the cluster loses several outer atoms during the initial stage of the impact, leaving only the core atoms of the cluster to participate in the implantation. The reason why this initial fragmentation was not typically seen in the simulations could be that the Ar atoms were equidistant in the model while in the real cluster cation there is a more compact (and strongly bound) core surrounded by outer-shell atoms with bonds which are only slightly stronger than conventional van der Waals ones. An additional reason for the fragmentation could be neutralization of the charged cluster: the cluster cation can capture an electron from the graphite surface at the very initial stage of the collision. The neutralization causes a deformation, leading to the cluster swelling and imparting lateral momenta to the outer atoms.

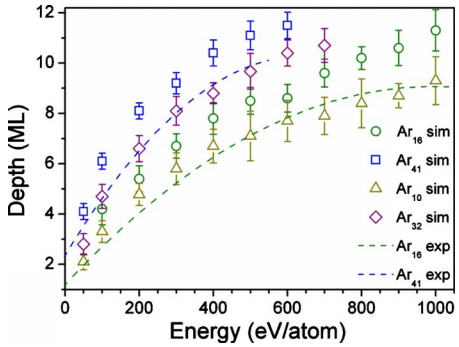

FIG. 4. (Color online) Simulated dependences of depth of deepest implanted Ar atoms on energy. For Ar_{16} and Ar_{41} bond length is shortened to 70% of that at equilibrium (van der Waals type). For Ar_{10} and Ar_{32} Ar-Ar distances are at equilibrium. Dashed lines show the experimental dependences [same as in Fig. 3(a)].

Possession of even small lateral momenta by the atoms of the outer shell can facilitate their escape from the cluster in the first collision with the target atoms at the surface and they do not participate further in the implantation. This assumption is supported by some simulations showing that if an atom departs from the cluster at the surface it has considerable lateral component of velocity and therefore stops between the uppermost graphene layers. To provide support for the fragmentation model, we simulated implantation of reduced-size clusters, Ar_{10} and Ar_{32}, using the unmodified neutral Ar-Ar interaction. As one can see in Fig. 4, the agreement with the experimental curves is very good. The mechanism of cluster rearrangement is found to be important mainly for small clusters and the influence of the initial charge state becomes insignificant for clusters greater than approximately 50 atoms.

In conclusion, data on the implantation of argon clusters shows a surprising similarity to the implantation behavior of metallic clusters and demonstrates the universality of a simple empirical scaling law for cluster implantation into graphite. It is worth noting that the linear dependence of cluster stopping on momentum is completely different compared to the stopping of monoatomic projectiles which linearly scales with energy. On the other hand, the proposed scaling law for cluster stopping creates a bridge to surface collisions of macroscopic bodies having their penetration depths linearly scaled with velocity. MD simulations indicate that the rare gas cluster implantation dynamics may be influenced by charge transfer and deformation induced in the early stages of the impact. However, the exact mechanism of the cluster rearrangement during the implantation is open and *ab initio* calculations are needed to investigate it more fully.

Two of the authors (V.N.P. and E.E.B.C.) are grateful for the financial support of the Swedish Research Council (Vetenskapsrådet). E.E.B.C. acknowledges support from the WCU program through KOSEF funded by MEST (Grant No. R31-2008-000-10057-0). The computational part of this work was performed within the Finnish Centre of Excellence in Computational Molecular Science (CMS), financed by The Academy of Finland and University of Helsinki.

*Present address: Institute of Physics, University of Rostock, 18051 Rostock, Germany; vladimir.popok@uni-rostock.de

[1] I. Yamada, J. Matsuo, N. Toyoda, and A. Kirkpatrick, Mater. Sci. Eng. R. **34**, 231 (2001).
[2] V. N. Popok and E. E. B. Campbell, Rev. Adv. Mater. Sci. **11**, 19 (2006).
[3] R. E. Palmer, S. Pratontep, and H.-G. Boyen, Nature Mater. **2**, 443 (2003).
[4] S. Vajda, M. J. Pellin, J. P. Greeley, C. L. Marshall, L. A. Curtiss, G. A. Ballentine, J. Elam, S. Catillon-Mucherie, P. C. Redfern, F. Mehmood, and P. Zapol, Nature Mater. **8**, 213 (2009).
[5] J. Borland, J. Hautala, M. Gwinn, T. G. Tetreault, and W. Skinner, Solid State Technol. **47**, 64 (2004).
[6] S. S. Datta, D. R. Strachan, S. M. Khamis, and A. T. C. Johnson, Nano Lett. **8**, 1912 (2008).
[7] V. N. Popok, S. Vučković, J. Samela, T. T. Järvi, K. Nordlund, and E. E. B. Campbell, Phys. Rev. B **80**, 205419 (2009).
[8] V. Popok, S. Prasalovich, and E. Campbell, Vacuum **76**, 265 (2004).
[9] Y. Yamamura, Nucl. Instrum. Methods Phys. Res. B **33**, 493 (1988).
[10] V. I. Shulga, M. Vicanek, and P. Sigmund, Phys. Rev. A **39**, 3360 (1989).
[11] S. Prasalovich, V. Popok, P. Persson, and E. Campbell, Eur. Phys. J. D **36**, 79 (2005).
[12] J. Samela and K. Nordlund, Phys. Rev. Lett. **101**, 027601 (2008).
[13] J. Samela, K. Nordlund, V. N. Popok, and E. E. B. Campbell, Phys. Rev. B **77**, 075309 (2008).
[14] J. F. Ziegler, J. P. Biersack, and M. D. Littmark, *The Stopping and Ranges of Ions in Matter* (Lulu Press, Morrisville, 2008).
[15] J. R. Baker, Int. J. Impact Eng. **17**, 25 (1995).
[16] V. N. Popok, S. V. Prasalovich, M. Samuelsson, and E. E. B. Campbell, Rev. Sci. Instrum. **73**, 4283 (2002).
[17] S. Vučković, M. Svanqvist, and V. N. Popok, Rev. Sci. Instrum. **79**, 073303 (2008).
[18] S. Pratontep, P. Preece, C. Xirouchaki, R. E. Palmer, C. F. Sanz-Navarro, S. D. Kenny, and R. Smith, Phys. Rev. Lett. **90**, 055503 (2003).
[19] L. Seminara, P. Convers, R. Monot, and W. Harbich, Eur. Phys. J. D **29**, 49 (2004).
[20] K. Nordlund, M. Ghaly, R. S. Averback, M. Caturla, T. Diaz de la Rubia, and J. Tarus, Phys. Rev. B **57**, 7556 (1998).
[21] M. Ghaly, K. Nordlund, and R. S. Averback, Philos. Mag. A **79**, 795 (1999).
[22] K. Nordlund, Comput. Mater. Sci. **3**, 448 (1995).
[23] K. Nordlund, J. Keinonen, and T. Mattila, Phys. Rev. Lett. **77**, 699 (1996).
[24] K. Nordlund, N. Runeberg, and D. Sundholm, Nucl. Instrum. Methods Phys. Res. B **132**, 45 (1997).
[25] K. Nordlund, J. Keinonen, and A. Kuronen, Phys. Scr. **T54**, 34 (1994).
[26] H. Haberland, B. von Issendorf, T. Kolar, H. Kornmeier, C. Ludewigt, and A. Rish, Phys. Rev. Lett. **67**, 3290 (1991).
[27] T. Ikegami, T. Kondow, and S. Iwata, J. Chem. Phys. **98**, 3038 (1993).
[28] N. L. Doltsinis, P. J. Knowles, and F. Y. Naumkin, Mol. Phys. **96**, 749 (1999).
[29] J. A. Gascón and R. W. Hall, J. Phys. Chem. B **105**, 6579 (2001).